Transactions, SMiRT-23
Manchester, United Kingdom - August 10-14, 2015
Division I, Paper ID 799

THE INFLUENCE OF LATERAL EXPANSIONS ON THE RESPONSE OF STEEL-CONCRETE COMPOSITE STRUCTURES

Trevor D. Hrynyk[1] and Frank J. Vecchio[2]

[1] Assistant Professor, Dept. of Civil, Arch. and Env. Engineering, University of Texas at Austin, U.S.A.
[2] Professor, Dept. of Civil Engineering, University of Toronto, Canada.

ABSTRACT

Steel-concrete (SC) composite wall elements are commonly employed in nuclear containment internal structures and are an appealing option for the construction of modern small modular reactors. Thus, there is a need for improved understanding of structural response mechanisms that are unique to SC wall elements and currently are not well understood. This paper presents the results from a series of nonlinear finite element analyses that were performed to examine the development and influence of material expansions on the response of SC composite elements. Constitutive modelling is done in accordance with an extended formulation of the Disturbed Stress Field Model (DSFM), a smeared rotating crack procedure shown to be capable of accurately capturing the behaviour of shear-critical conventionally reinforced concrete elements under general loading conditions. The results from the analytical study show that lateral restraint effects stemming from differential expansions of the steel faceplates and the concrete cores comprising SC elements play a major role in computed capacity and response. The sensitivity of the computed SC element response to analysis parameters and material properties that are often assumed in computational modelling procedures (e.g., Poisson's ratios used) is examined and discussed.

INTRODUCTION

Steel-concrete (SC) composite walls are structural elements comprised of thick concrete core sections sandwiched between comparatively thin steel faceplates. The concrete thicknesses of these elements can be in the order of several feet (approximately one metre) while the steel faceplates thickness may be less than one inch (in the range of two to three centimetres). SC wall elements typically contain no conventional in-plane reinforcement (i.e., no horizontal or vertical reinforcing bars) and no conventional shear reinforcement (i.e., no through-thickness stirrups or headed bars) and the faceplates are connected to the core using steel shear stud connectors and full depth cross-tie bars. In addition to providing anchorage, cross-tie bars are also used as out-of-plane shear reinforcement.

Relative to conventional reinforced concrete structures, the modular nature of SC composite wall elements can be well-suited for efficient construction practice. The prefabricated steel shells serving as the primary steel reinforcement of SC elements also function as the formwork used during the concrete casting process. Over the past several decades, there has been extensive research focused toward evaluating the feasibility of using SC systems in the construction of nuclear power plant structures in an effort to reduce costs (Braverman et al. 1997) and to improve structural performance under extreme loading conditions. As a result, to date the most common application of SC wall elements has been in the construction of nuclear containment internal structures (Varma et al. 2014). Furthermore, SC construction is now also being considered as a potentially viable option for the construction of modern concept small modular reactors.

In comparison to the large volume of experimental work that has been carried-out to investigate the performance of SC composite wall elements, research focused toward the development and application of reliable SC modelling procedures is relatively scarce. From the limited work that has been performed in

this area, the majority of the analytical and computational procedures used to model SC structure response can generally be subdivided into two approaches: i) idealized strut-and-tie models which have met with some success for member level design and assessment applications and ii) finite element analysis procedures which have been more commonly employed in system level SC infrastructure applications. In the case of finite element procedures, the typical approach used to model SC structures has been to employ powerful general purpose computational software packages to develop a micro-model representation of the structure or substructure under consideration. Such modelling procedures require extremely fine meshing techniques, typically involving the explicit representation of each individual shear stud and tie-bar comprising the structure, and most often employ dense distributions of solid finite elements to create some form of three-dimensional continuum. The successes of this approach have been somewhat limited as not only are such procedures computationally expensive, but many of the available commercial software packages that have been used for these investigations rely on concrete constitutive formulations based on classical solid mechanics concepts with material relations developed from test data pertaining to small-scale unreinforced and uncracked concrete elements. Thus, for computational investigations focused on the performance of large-scale SC composite wall structures, the application of simple finite element modelling procedures employing behavioural models that have been shown to adequately capture the response of cracked reinforced concrete elements under a broad range of loading conditions, should be viewed as an equally viable, if not an improved, computational approach for assessing SC structure response.

In this paper, nonlinear finite element modelling is used to examine the influence of passive lateral stresses attributed to differential expansions of the concrete core and steel faceplates comprising SC composite wall elements. Cracked SC element behavioural modelling is done on the basis of the formulations of the Disturbed Stress Field Model (DSFM) (Vecchio 2000), an advanced reinforced concrete behavioural model developed as an extension of the Modified Compression Field Theory (MCFT) (Vecchio and Collins 1986). This smeared crack analysis procedure inherently considers the redistribution of internal forces that can occur due to local changes in stiffness arising from cracking or crushing of concrete, yielding of the steel faceplates, the effect of variable and changing crack widths (including slip deformations along crack surfaces), and various second-order mechanisms that can contribute to the response of cracked reinforced concrete structures. As adapted to accommodate SC wall element construction, the DSFM-based procedure has been implemented within the framework of a layered ‘thick-shell’ nonlinear finite element program (Hrynyk and Vecchio 2015). Unlike commercial analysis programs that typically require complex and expensive meshing procedures, the layered shell element approach considered in these analyses can capture complex structure response (including through-thickness shearing effects) using basic finite element modelling techniques requiring significantly reduced computational effort. This feature, combined with the advanced behavioural modelling employed, makes the layered ‘thick-shell’ element approach more practical for investigation of large-scale SC structures that may be subjected to in-plane loads, out-of-plane loads, or scenarios involving combined in-plane and out-of-plane loads. The influence of lateral expansions on the response of SC composite wall elements is examined using both in-plane and out-of-plane loading scenarios.

MODELLING OF SC COMPOSITES

The smeared crack modelling procedure used for investigation of SC composite wall element response is based principally on the two-dimensional plane stress analysis procedure presented by Vecchio and McQuade (2011). Steel faceplates are explicitly represented in the layered shell element and, in accordance with the modified thick-shell formulation employed (Hrynyk and Vecchio 2015), are subject to plane sections strain compatibility through the thickness. The layered discretization of the SC shell element and associated material stress and strain response characteristics are presented in Figure 1.

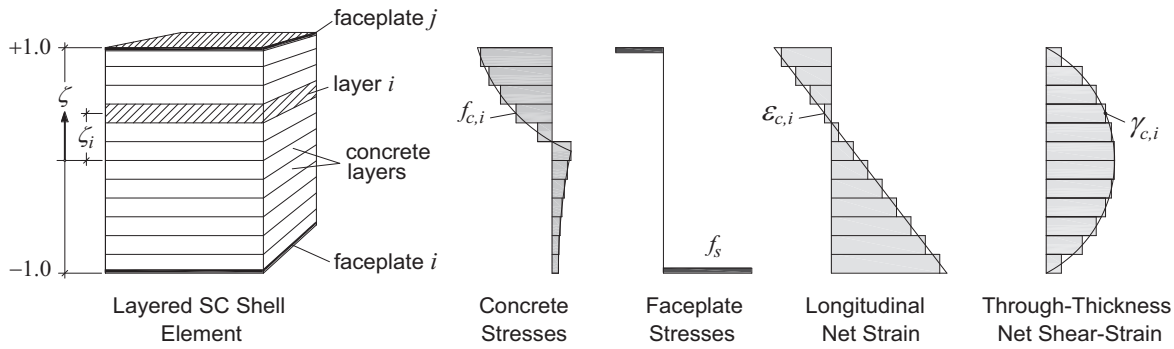

Figure 1. Multilayer 'thick-shell' SC element

Faceplate Constitutive Modelling

Constitutive modelling of the steel faceplates was done in accordance with the trilinear model proposed by Seckin (1981) which incorporates the Bauschinger effect. The von Mises yielding criterion (refer to Equation 1) was used to estimate the response of the steel faceplates under biaxial stress states. Note that because the parabolic out-of-plane (through-thickness) shear strain distribution considered in the layered analysis procedure results in small, arguably negligible, out-of-plane shear strains at the surfaces of the elements (refer to Figure 1), it is assumed that the steel faceplates are subjected to in-plane stress conditions only. Note that for typical SC construction scenarios involving comparatively thin steel faceplates relative to their thick concrete core sections, the out-of-plane shear forced carried by the steel faceplates are likely to be negligible.

$$\left(f_{s1}-f_{s2}\right)^2+\left(f_{s2}-f_{s3}\right)^2+\left(f_{s3}-f_{s1}\right)^2=2\left(f_y\right)^2 \tag{1}$$

In the above equation f_{s1}, f_{s2}, and f_{s3} represent the principal stresses in the faceplate. Note however, with the assumption that the steel faceplates are limited to in-plane stress conditions, one of the three principal stresses in the plate will always be zero.

Two buckling models are used to consider steel faceplate buckling: i) the modified Euler elastic buckling expression originally presented by Usami et al. (1995) (refer to Equation 2), and ii) a refinement of the post-buckling steel stress degradation model originally presented by Dhakal and Maekawa (2002a,b) for conventional steel reinforcing bars (refer to Equation 3). In the model developed by Usami et al. (1995), the critical elastic buckling stress (σ_{cr}) of steel faceplates with stud spacing to plate thickness ratios of b/t_s is approximated using the following modified Euler expression:

$$\sigma_{cr}=\pi^2 E_s/[12n^2(b/t_s)^2] \tag{2}$$

where n = 0.7 and E_s is the modulus of elasticity of the steel faceplates. The refined Dhakal-Maekawa model is used to supplement the Usami elastic buckling model presented above and to provide an estimate of the post-buckled stress-strain response of the steel faceplates. Once plate buckling is estimated to occur, the post-buckled compressive stress, f_i, is estimated using the following relationship:

$$\frac{f_i}{f_y}=\left[1.1\text{-}0.016\sqrt{\frac{f_y}{10}}\cdot\frac{L}{D}\right]\left[0.8+1.8\frac{f_u}{f_y}\cdot\frac{D}{L}\right] \quad \text{for} \quad \frac{f_i}{f_y}\le\frac{f_{it}}{f_y}, \text{ otherwise } \frac{f_i}{f_y}=\frac{f_{it}}{f_y} \tag{3}$$

where for the purpose of the faceplates comprising SC composite wall elements, f_y is the absolute minimum of the yield stress of the plate or the elastic plate buckling stress provided by Equation 2. L is taken as the length between the shear stud connectors, D is the thickness of the plate, f_u is the ultimate strength of the plate, and f_{it} is the tensile stress corresponding to strain ε_i.

Assumptions

In agreement with the modelling approach previously employed by Vecchio and McQuade (2011), several assumptions have been made regarding steel faceplate-concrete core interaction mechanisms that are currently not well understood. Specifically, it was assumed that:

i) Steel faceplate contribution toward concrete tension stiffening is negligible.
Tension stiffening effects in conventional reinforced concrete members are often only considered effective for concrete regions located within some tributary distance of a deformed steel reinforcing bar (refer to Figure 2). The *fib* Model Code (CEB-FIP 1990) would suggest that this tributary distance is a function of the reinforcing bar diameter. As the tension stiffening effect is primarily attributed to bond related mechanisms developed between deformed bars and concrete, it is unknown to what degree, if any, tension stiffening effects will be developed by way of smooth steel faceplates that are stud-anchored to concrete. Moreover, relative to the faceplates, the thicknesses of the concrete core sections typically used in SC construction applications are large. Thus, even if bond related tensile stresses are developed, conventional methods of evaluating the effective tension stiffened regions would suggest that the majority of the concrete core would remain unaffected.

ii) Average crack spacing of SC elements is approximately equal to the total element thickness.
Several crack spacing models have been proposed for conventional reinforced concrete elements containing deformed and/or smooth steel reinforcing bars. In the DSFM, average crack spacings are used to evaluate average crack widths. The influences of variable and changing crack widths bear heavily on the local element response considered in the DSFM. Additionally, element crack spacings and crack widths can also bear heavily on the post-cracking tensile stress degradation of unreinforced concrete elements, a significant consideration given that tension stiffening effects are neglected in the procedure considered (refer to Figure 2b).

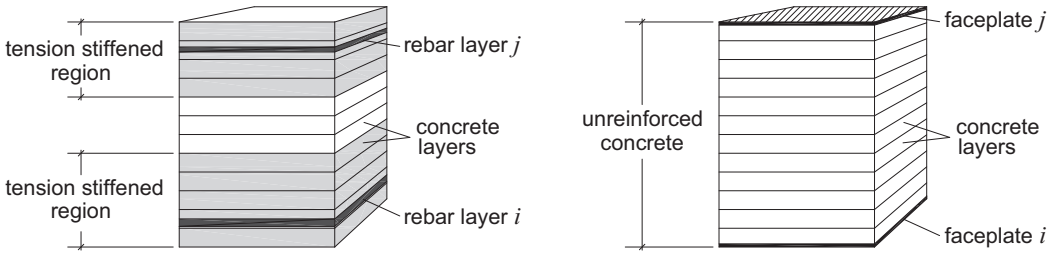

(a) conventional RC element (b) SC shell element

Figure 2 – Consideration of tension stiffening effects.

In North-American reinforced concrete code provisions (CSA 2004; AASHTO 2014), the maximum crack spacing is limited to the distance between layers of crack-control reinforcement. Where none is provided other than the primary flexural reinforcement, the maximum crack spacing is set as the effective depth of the member. Thus, it has been assumed that the maximum crack spacing for SC elements can be approximated as being equal to the overall through-thickness depth of the element (centre-to-centre distance between faceplates).

iii) Shear stud connectors are sufficient in both size and density to prevent interfacial slip.
Lastly, to simplify initial development of the analysis procedure, interfacial slip attributed to insufficient anchorage provided between the steel faceplates and the concrete core is neglected. Thus, stiffness and strength reductions attributed to interfacial slip are not captured.

Assumptions (i) and (ii) above are believed to be relatively conservative. However, with the absence of data from experimental investigations targeted toward investigating the cracking behaviour and post-cracking tensile stress resistance of SC elements, the use of less conservative or possibly more favourable modelling assumptions is not warranted. For an SC element containing no conventional reinforcement (e.g., no deformed steel reinforcing bars), assumption (i) above considers the core concrete section in a manner directly analogous to that of plain unreinforced concrete. Given the large crack spacings that are considered in the analysis procedure, post-cracking concrete tensile stresses of SC elements are estimated to diminish abruptly and almost immediately after cracks first develop in the concrete.

LATERAL STRESS DEVELOPMENT IN SC COMPOSITES

The in-plane force interaction of an arbitrary SC element subjected to monotonically increasing biaxial stress conditions was investigated using the DSFM-based analysis procedure described above. The interaction behaviour was developed for a 915 mm-thick SC wall element with 19 mm-thick steel faceplates. The peak compressive strength of the concrete was 41.4 MPa and the yield stress of the faceplates was 345 MPa. The finite element mesh consisted of four SC shell elements in a 2 x 2 grid with three layers comprising each element (one for the concrete core, and two for the faceplates) (refer to Figure 3a). The response of this specific SC element has been used previously for SC analytical investigations by others (Varma et al. 2011a).

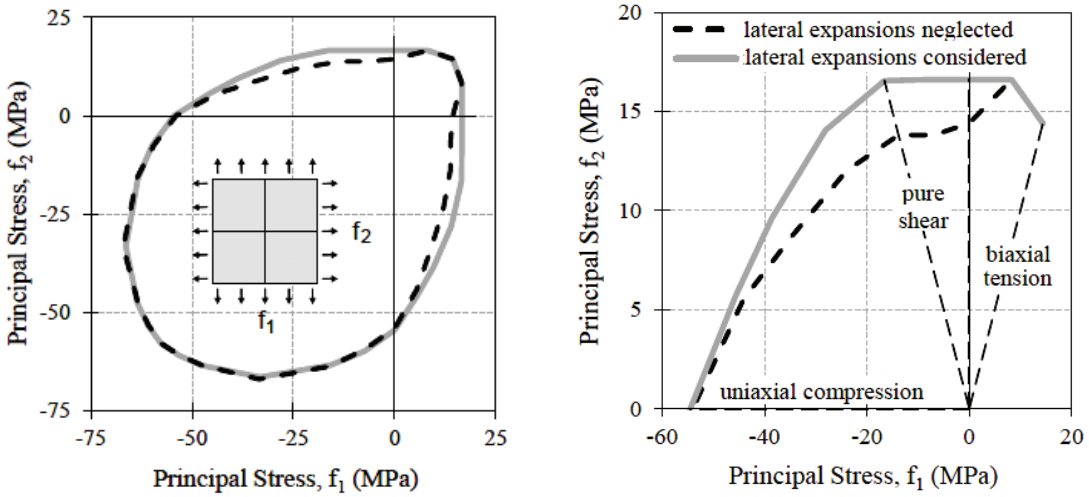

(a) full biaxial response (b) tension-compression loading regime

Figure 3 – Computed SC in-plane interaction response.

The role of lateral stresses developed as a result of the composite action between the steel faceplates and the concrete core on the computed strength interaction response of the trial SC element is presented in Figure 3. It is apparent that, in this case, the restraint of lateral deformations that were estimated to occur due to Poisson's effect and concrete dilatation led to increased SC element strength estimates throughout the majority of the tension-compression region of the biaxial strength envelope. Under biaxial compression and biaxial tension loading scenarios, material expansions were found to be of less significance. This effect is perhaps more apparent when one considers the simple case of an SC element

under in-plane uniaxial tension: as axial tensile forces are applied to the composite element and axial tensile stresses are developed in the faceplates, the Poisson effect in the steel leads to the development of lateral deformations which, if unrestrained, would cause the faceplates to contract in the lateral directions. However, due to small tensile stresses (potentially zero for SC type elements) developed in the concrete after cracking, it has been assumed that the cracked concrete core under axial tension does not exhibit the Poisson related lateral contraction that is typically associated with elastic materials (i.e., it is assumed that $v_c = 0$ for cracked concrete under tension). As a result, the stud-anchored concrete core of the SC element is estimated to restrain the steel faceplates, preventing them from contracting laterally and inducing lateral tension in the steel which in turn induces lateral compression in the concrete. Thus, even under uniaxial loading conditions the faceplates and concrete core are expected to experience biaxial stress conditions as a result of differential material expansion. In cases where confining effects or multi-axial yield criteria are considered (e.g., the von Mises yield criterion in the case of the steel faceplates), the degree of lateral expansion considered in the analysis will impact element capacity estimates.

The development of this form of passive confinement is dependent on the bond behaviour between the faceplates and the concrete core, and also on their respective Poisson ratios. In Figure 3 the capacity envelope (solid line) of the SC composite wall element was computed using assumed Poisson ratios of 0.15 for concrete (due to principal compression) and 0.30 for the steel faceplates. From the dashed line presented in the figure, it can be seen that when expansions due to Poisson's effect are neglected entirely (i.e., $v_c = v_s = 0$), a significant decrease in the computed capacity of the SC element is attained throughout the tension-compression loading region. Thus, for SC structure analyses, some level of care should be taken in specifying material expansion properties, particularly for elements subjected to shear dominated loading conditions. Furthermore, in cases where interfacial slip is likely to occur, it is possible that material expansions may result in only limited or negligible lateral stress development.

IMPLICATIONS FOR SC STRUCTURE RESPONSE

To examine the influence of expansion related lateral stresses in SC structural elements, nonlinear finite element analyses of SC members were performed using different Poisson's ratios for the concrete cores and the steel faceplates comprising SC structural elements. Analysis cases with Poisson expansions neglected entirely are performed to represent conditions where the occurrence of interfacial slip pre-empts the development of expansion related lateral stresses. Two types of SC structural elements have been considered: i) SC shear walls with details in accordance with the walls tested by Sasaki et al. (1995), and ii) SC beam-type elements that were modelled with the details reported by Varma et al. (2011b). In addition to the faceplate constitutive modelling procedures presented in this paper, supplemental material models identified in Hrynyk (2013) were used to supplement the DSFM-based analysis procedure.

Sasaki et al. SC Shear Walls

Sasaki et al. (1995) reported test results from a series of flanged SC shear walls under in-plane lateral cyclic loading. The walls were constructed with variable heights (ranging from 1250 to 2500 mm) and variable web thicknesses (ranging from 115 to 345 mm). The seven walls comprising the experimental program encompassed a broad range of design and testing variables: the ratio of bending moment to shear force applied, the steel-plate reinforcement ratio provided, the level of axial compression applied, and the shear stud details provided for the web-flange connection regions. However, the documented damage development was essentially common for all of the SC walls: following some initial cracking in the flange and web sections, the faceplates comprising these sections yielded and were reported to buckle, ultimately controlling capacity. The SC shear walls were modelled using a combination of layered shell and truss bar finite elements. As the shear walls in the testing program were subjected to pure in-plane loading conditions, the finite element models were also limited to planar deformations by restraining all rotational and out-of-plane translational degrees of freedom associated with the layered SC shell

elements. Three material layers were used for the SC shell elements employed: one concrete core layer and two layers representing the steel faceplates. The faceplates and bending stiffeners comprising the flanges of the walls were modelled using truss bar elements. Boundary members at the bases of the walls were fully fixed using a series of pinned nodal restraints. Loading of the upper boundary element was done in a displacement controlled manner and, for the purpose of this investigation, was done monotonically without cycling. For brevity, computational response estimates for only two of the seven walls are presented and were done using different values Poisson's ratios for the concrete and the steel faceplates.

The computed response estimates for SC wall H07T10 are presented in Figure 4. From the strain contour presented in Figure 4a, it can be seen that, at ultimate, the compressive strains of the SC wall were found to localize at the base of the web, at the web-flange intersection region of the wall. Steel plate yielding followed by concrete crushing within this region was estimated to result in an abrupt reduction in shear resistance. In agreement with that reported, web plate buckling was estimated to occur prior to the onset of concrete crushing. The computed failure mode was common for all Poisson's ratio values considered. From Figure 4b, it can be seen that, in all cases, assumptions made regarding the Poisson's ratios for the concrete and the steel faceplates had no apparent effect on the computed pre-peak stiffness of the SC shear wall. However, it was found that lateral expansions did influence wall capacity, with wall strength having the tendency to decrease with the level of steel lateral expansion considered. When the lateral expansions were neglected entirely, it resulted in the lowest estimates of capacity and post-peak stiffness.

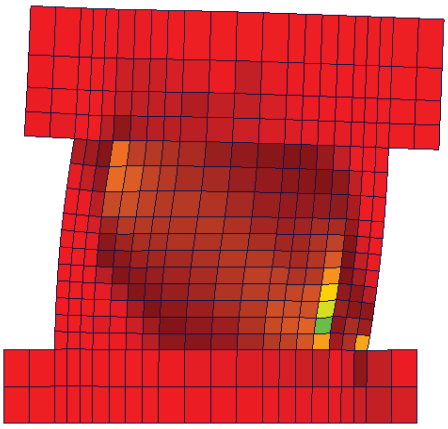

(a) principal compressive strain contour and displaced shape [x20] at ultimate ($\nu_c = 0.30$, $\nu_s = 0.15$)

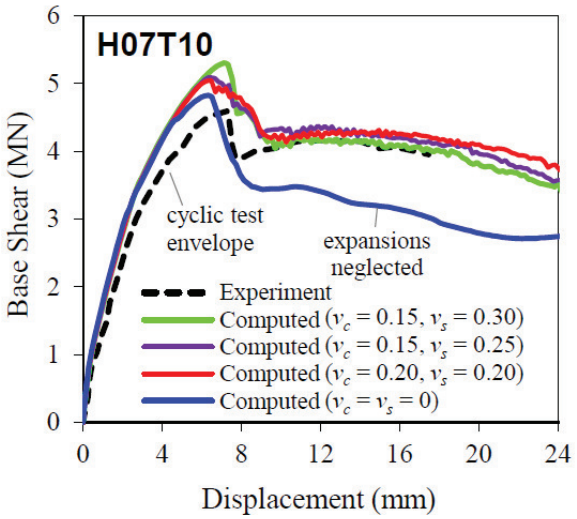

(b) load-displacement response

Figure 4 – Computed results for Sasaki shear wall H07T10 ($\rho_s = 2.00\,\%$; $t_{web} = 230$ mm; $h_{web} = 1{,}250$ mm).

From Figure 5, it can be seen that similar findings were found from the investigation of SC wall H10T10. Again, the Poisson's ratio values considered were found to influence computed wall capacity. The post-peak response of the wall was generally unaffected by the different Poisson's ratios values considered; however, was significantly influenced when lateral expansions were neglected entirely. In this case, the computational results tended to overestimate the experimentally reported capacity and the pre-peak stiffness of the SC wall immediately prior to failure. The pre-peak softening observed experimentally may have been affected by steel-concrete interfacial slip which was not explicitly considered in the analysis procedure employed. Additionally, the cycled loading protocol considered in the testing program is expected to have also contributed to structure softening that was not captured in the computational monotonic loading analyses performed.

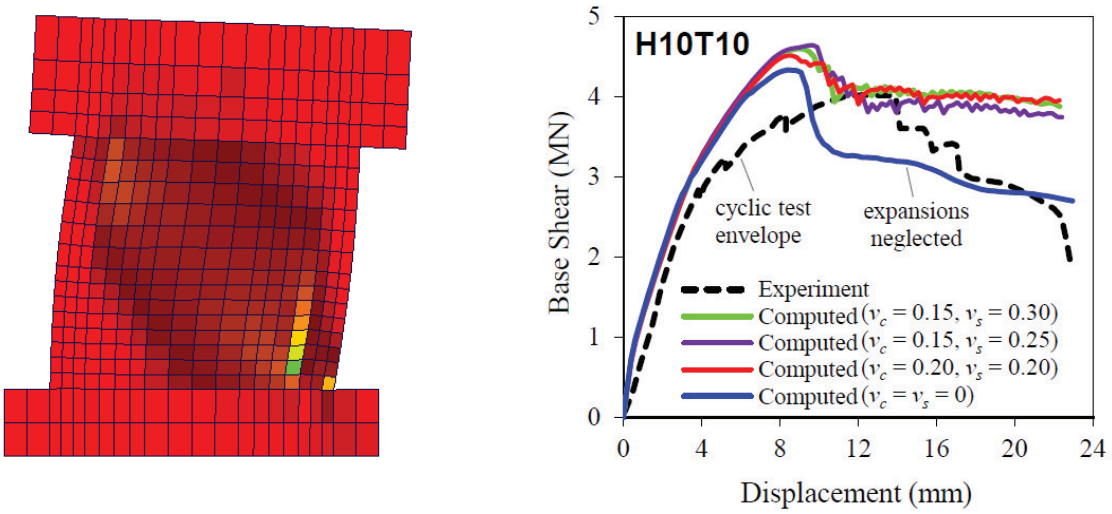

(a) principal compressive strain contour and displaced shape [x20] at ultimate (v_c = 0.30, v_s = 0.15)

(b) load-displacement response

Figure 5 – Computed results for Sasaki shear wall H10T10 (ρ_s = 2.00 %; t_{web} = 230 mm; h_{web} = 1,660 mm).

Varma et al. SC Beams

Varma et al. (2011b) presented details regarding an experimental testing program focused on investigating the response of SC beams subjected to out-of-plane shear forces. The SC beams comprising the program possessed different shear span to depth (a/d) ratios, faceplate thicknesses, shear stud configurations, and were constructed with or without through-thickness tie-bars. The research program included the testing of four full-scale SC beam members that were approximately 915 mm deep. Three of the four SC beams contained through-thickness shear reinforcement provided in the form of tie-bars that were 19 mm in diameter and were regularly spaced at 432 mm intervals, resulting in an out-of-plane reinforcement ratio of 0.15 %. The beams were subjected to four-point monotonic loading conditions.

Half-span models consisting of eight SC shell elements for the shortest beam (SP2-2), ten shell elements for the intermediate length beams (SP1-5 and SP2-1), and twelve shell elements for longest beam (SP2-3) were created. In all cases, element sizing was typically in the order of 40 to 50 % of the overall beam depth. The SC shell elements were subdivided into 40 equal thickness concrete layers. An additional two material layers were used to represent the steel faceplates located on the surfaces of the elements (see Figure 6) and out-of-plane shear reinforcement was treated as a smeared property within the concrete core layers. The 152 mm-length shear studs used to anchor the faceplates to the core were not included in the finite element models developed and, as such, local confining effects potentially provided by way of the studs have been neglected. A line of vertical nodal restraints across the widths of the beams were used to represent the end support reaction and axial and rotational restraints provided at the midspan locations of the beams were used to enforce symmetry. Loads were applied in a displacement controlled manner using an increment of 0.50 mm for all beams with the exception of the longest beam, beam SP2-3, which was loaded using displacement increments of 1.00 mm. In all cases member self-weight was neglected.

For brevity, the computed total load-displacement responses for the two of the four large-scale SC beams have been plotted alongside the experimental results in Figure 7. It can be seen that the analyses captured the initial stiffnesses, capacities, and failure modes of the SC beams with reasonable levels of accuracy. In agreement with that reported in the testing program, a brittle shear failure mode was estimated to occur for beam SP2-1 (a/d = 3.5) (see Figure 7a) and a ductile flexurally-governed failure mode was computed for beam SP2-3 (a/d = 5.5). In both cases, the ultimate shear capacities were marginally overestimated

when lateral expansions were considered; however, remained within approximately 9 % of those reported. From Figure 7b it can be seen that regardless of the lateral expansion considered, the analysis procedure captured the flexural failure mode for SC SP2-3; however, the lateral expansions considered significantly influenced computed ductility. For the two SC beams presented, faceplate yield strength enhancement resulting from lateral restraint effects and the von Mises yield criterion was estimated to play a significant role in the computed shear capacities of the beams. This enhanced yield strength is particularly evident from the hardening response exhibited by beam SP2-3 throughout the 50 to 70 mm displacement range. In this case, the Poisson's ratios used for the SC element materials and the perfect bond assumption between the steel faceplates and the concrete are shown to be contributors to the overestimation of SC beam strength and led to reduced displacement capacity.

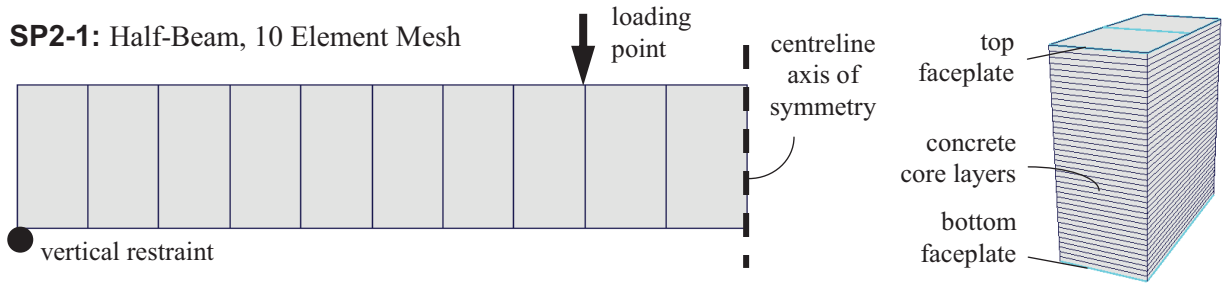

(a) elevation of finite element mesh (b) layered discretization

Figure 6 – Finite element mesh for Varma SC beam SP2-1 ($\rho_s = 2.10\,\%$; a/d = 3.5; L = 10,060 mm).

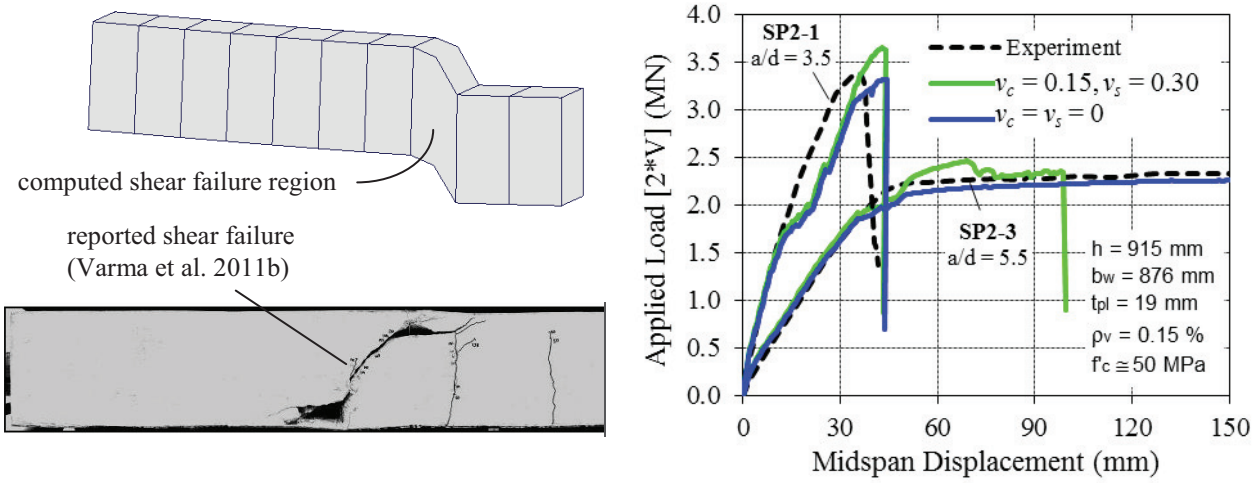

(a) shear failure mode for SC beam SP2-1 (b) load-deflection responses for SP2-1 and SP2-3

Figure 7 – Computed results for Varma et al. SC beams

CONCLUSIONS

In this paper, nonlinear finite analyses were used to examine the influence of lateral expansions and restraint effects on the performance of SC composite wall elements. On the basis of the results presented, the following conclusions are drawn:

- The smeared crack DSFM-based SC composite element modelling approach can be used in the framework of a 'thick-shell' finite element procedure to examine the behaviour of SC structures subjected to three-dimensional loading conditions involving in-plane and out-of-plane shear.

- Poisson's effect was found to contribute to the computed load resisting behaviours of SC elements. Differential lateral expansion experienced by the steel faceplates and the concrete cores comprising the SC elements produced a form of passive confinement. Varying the Poisson's ratio used for the steel faceplates and the concrete core was shown to influence computed strength and deformation capacities of SC composite members.
- Stresses developed by way of lateral expansions are contingent on the composite action of the SC faceplates and the concrete core. Thus, care should be taken in assessing the performance of SC structures in cases where interfacial slip is expected to occur.

REFERENCES

AASHTO (2014). "LRFD Bridge Design Specifications", Seventh Edition, American Association of State Highway and Transportation Officials, Washington, DC, USA, 1704 pp.

Braverman, J., Morante, R., Hofmayer, C., and Graves, H., (1997). "The Use of Concrete-Filled Steel Structures for Modular Construction of Advanced Reactors". Brookhaven National Laboratory / U.S. Nuclear Regulatory Commission, Report No. BNL-NUREG-64172, April, 8 pp.

Comité EURO-International du Béton. (1990). "Model code for concrete structures." *CEB-FIP MC90*.

CSA A23.3 (2004). "Design of Concrete Structures", Canadian Standards Association, Mississauga, Ontario, Canada, 214 pp.

Dhakal, R.P., Maekawa, K. (2002a). "Modeling for post-yield buckling of reinforcement", ASCE J. Struct. Eng., Vol. 128, No. 9, pp. 1139-1147.

Dhakal, R.P., Maekawa, K. (2002b). "Reinforcement Stability and Fracture of Cover Concrete in Reinforced Concrete Members", ASCE J. Struct. Eng., Vol. 128, No. 10, pp. 1253-1262.

Hrynyk, T.D. (2013). "Behaviour and Modelling of Reinforced Concrete Slabs and Shells Under Static and Dynamic Loads", Ph.D. Dissertation, University of Toronto, Dept. of Civil Engineering, 455 p.

Hrynyk, T.D., and Vecchio, F.J. (2015). "Capturing Out-of-Plane Shear Failures in the Analysis of Reinforced Concrete Shells", accepted for publication in ASCE J. Struct. Eng.

Sasaki, N., Akiyiama, H., Narikawa, M., Hara, K., Takeuchi, M., and Usami, S. (1995). "Study on a Concrete Filled Steel Structure for Nuclear Power Plants - Part 3: Shear and Bending Loading Tests on Wall Member", *SMiRT 13*, Porto Alegre, Brazil, August, pp. 27-32.

Seckin, M. (1981). "Hysteretic Behavior of Cast-in-Place Exterior Beam-Column-Slab Subassemblies", Ph.D. Diss., University of Toronto, Department of Civil Engineering, 266 pp.

Usami, S., Akiyama, H., Narikawa, M., Hara, K., Takeuchi, M., and Sasaki, N. (1995). "Study on a Concrete Filled Steel Structure for Nuclear Power Plants - Part 2: Compressive Tests on Wall Members, SMiRT 13, Porto Alegre, Brazil, August, pp. 21-26.

Varma, A.H., Malushte, S.R., Sener, K., Lai, Z. (2011a). "Steel-Plate Composite (SC) Walls for Nuclear Safety Related Nuclear Facilities: Design for In-Plane and Out-of-Plane Demands", SMiRT 21, Paper ID # 760, New Delhi, India, November, 8 pp.

Varma, A.H., Sener, K.C., Zhang, K., Coogler, K., Malushte, S.R. (2011b). "Out-of-Plane Shear Behavior of SC Composite Structures", SMiRT 21, Paper ID # 763, New Delhi, India, November, 8 pp.

Varma, A. H., Malushte, S., Sener, K., and Lai, Z. (2014). "Steel-plate composite (SC) walls for safety related nuclear facilities: Design for in-plane force and out-of-plane moments", Nuclear Engineering & Design, Vol. 269, pp. 240–249.

Vecchio, F.J. (2000). "Disturbed Stress Field Model for Reinforced Concrete: Formulation", ASCE J. Struct. Eng., Vol. 126, No. 9, pp. 1070-1077.

Vecchio, F.J., and Collins, M.P. (1986). "The Modified Compression Field Theory for Reinforced Concrete Elements Subjected to Shear", J. ACI, Vol. 83, No. 2, pp. 219-231.

Vecchio, F.J. and McQuade, I. (2011). "Towards improved modelling of steel-concrete composite wall elements", Nuclear Engineering and Design, Vol. 241, pp. 2629-2642.

Vecchio, F.J. and McQuade, I. (2011). "Towards improved modelling of steel-concrete composite wall elements", Nuclear Engineering and Design, Vol. 241, pp. 2629-2642.